Society For Biomaterials

Characterizing natural hydrogel for reconstruction of three-dimensional lymphoid stromal network to model T-cell interactions

Jiwon Kim,[1] Biming Wu,[2] Steven M. Niedzielski,[3] Matthew T. Hill,[2] Rhima M. Coleman,[2] Akira Ono,[4] Ariella Shikanov[1,2]

[1]Department of Macromolecular Science and Engineering, University of Michigan, Ann Arbor, Michigan
[2]Department of Biomedical Engineering, University of Michigan, Ann Arbor, Michigan
[3]Department of Chemical Engineering, University of Michigan, Ann Arbor, Michigan
[4]Department of Microbiology and Immunology, University of Michigan, Ann Arbor, Michigan

Received 18 September 2014; revised 21 January 2015; accepted 27 January 2015
Published online 15 February 2015 in Wiley Online Library (wileyonlinelibrary.com). DOI: 10.1002/jbm.a.35409

Abstract: Hydrogels have been used in regenerative medicine because they provide a three-dimensional environment similar to soft tissues, allow diffusion of nutrients, present critical biological signals, and degrade via endogenous enzymatic mechanisms. Herein, we developed *in vitro* system mimicking cell–cell and cell–matrix interactions in secondary lymphoid organs (SLOs). Existing *in vitro* culture systems cannot accurately represent the complex interactions happening between T-cells and stromal cells in immune response. To model T-cell interaction in SLOs *in vitro*, we encapsulated stromal cells in fibrin, collagen, or fibrin–collagen hydrogels and studied how different mechanical and biological properties affect stromal network formation. Overall, fibrin supplemented with aprotinin was superior to collagen and fibrin–collagen in terms of network formation and promotion of T-cell penetration. After 8 days of culture, stromal networks formed through branching and joining with other adjacent cell populations. T-cells added to the newly formed stromal networks migrated and attached to stromal cells, similar to the T-cell zones of the lymph nodes *in vivo*. Our results suggest that the constructed three-dimensional lymphoid stromal network can mimic the *in vivo* environment and allow the modeling of T-cell interaction in SLOs. © 2015 Wiley Periodicals, Inc. J Biomed Mater Res Part A: 103A: 2701–2710, 2015.

Key Words: natural hydrogels, three-dimensional (3D) cell culture, fibrin, secondary lymphoid organs, stromal network

How to cite this article: Kim J, Wu B, Niedzielski SM, Hill MT, Coleman RM, Ono A, Shikanov A. 2015. Characterizing natural hydrogel for reconstruction of three-dimensional lymphoid stromal network to model T-cell interactions. J Biomed Mater Res Part A 2015:103A:2701–2710.

INTRODUCTION

Secondary lymphoid organs (SLOs) suppress spread of pathogens in the host body, induce an efficient antimicrobial immune response by promoting contact between antigen-presenting cells and lymphocytes, and promote the survival and differentiation of lymphocytes.[1] CD4+ and CD8+ T-cells and stromal cells play an essential role in these functions, and they are densely packed in the paracortex of the lymph nodes and the interfollicular zone of Peyer's patches, which are called "T-cell zones."[1] The stromal cells, which include fibroblastic reticular cells (FRCs) and lymphatic endothelial cells, function in the initiation and maintenance of immune responses by directing circulation of naive T-cells through the paracortical regions.[2,3] In addition to the function of the individual stromal cells, the highly specialized microarchitecture of the stromal network contributes to primary immune response by spatially separating T-cell zones composed of stromal cells that control T-cell migration via chemokines from other compartments.[4] Multiple *in vivo* imaging studies[5,6] have reported that the stromal network provides a structural basis that supports maximum cell-to-cell communication while maintaining T-cell motility.[2]

Cells interact in a bidirectional and dynamic manner with extracellular matrix (ECM) components of the tissues *in vivo*.[7] Natural hydrogels, such as fibrin and collagen, can mimic complex physiological ECM environments. In this study, we investigated whether natural hydrogels can mimic the three-dimensional (3D) stromal network *in vitro* with which we can model T-cell behavior and functions in SLOs. These hydrogels provide a mechanical and biochemical environment and allow interaction among embedded cells because of their endogenous biological activity. Fibrin gel, which is the main component found in blood clots, has been characterized extensively as a plausible 3D hydrogel for

Additional Supporting Information may be found in the online version of this article.
Correspondence to: A. Shikanov; e-mail: shikanov@umich.edu
Contract grant sponsor: University of Michigan MCubed Seed Fund
Contract grant sponsor: Tissue Engineering and Regeneration (TEAM) Grant; contract grant number: NIH T32 DE007057 (to J.K.)

© 2015 WILEY PERIODICALS, INC.

various tissue-engineering applications.[8,9] Cell-secreted enzymes, such as plasmin and matrix metalloproteinases, can degrade fibrin and allow cell migration, proliferation, and remodeling of the encapsulating matrix.[10] Another alternative that has been widely used in the 3D cell culture is collagen. Collagen is the main component of ECM in many tissues and has been used as a 3D culture system because of its structural integrity.[11–14]

Understanding T-cell interactions has important implications in understanding the immune response and viral transmission. For example, T-cells are known natural hosts of human immunodeficiency virus (HIV)-1, the causative agent of acquired immunodeficiency syndrome. When infected, T-cells make contact with uninfected T-cells, and HIV-1 particles get transmitted by cell-to-cell transmission.[15,16] In a patient's body, this is most likely to occur in lymphoid organs where networks of ECM and stromal cells regulate T-cell behavior.[3] *In vitro* studies for viral transmission in SLOs have adopted two-dimensional cell-to-cell viral transfer assays in co-culture system.[15,16] However, multiple reports have shown that the microenvironment modulates cell morphology, cellular behaviors,[11,17] and lymphocyte migration.[18] Multiphoton imaging has provided some insight on the effects of microenvironment on viral spread *in vivo*[19] although it remains challenging to elucidate the molecular determinants involved in behaviors of infected T-cells in these approaches.

The needs for understanding the functions of T-cells in lymphoid organ microenvironment are increasing, yet there are no tractable *in vitro* systems that allow dissection of T-cell behavior and functions in such microenvironment. Previous studies on T-cell migration *in vitro* used fibronectin-coated surfaces[20] or 3D collagen matrices,[21] but focused mainly on the migratory behavior of lymphocytes and did not account for the presence of stromal networks. It has been shown that T-cell migration and trafficking depend on CC-chemokine ligand 19 (CCL19) and CCR 21 that are expressed by stromal cells.[2] To better mimic the *in vivo* microenvironment, we first built the stromal network by encapsulating stromal cells derived from human bone marrow in 3D hydrogels and allowing cells to proliferate and remodel their environment. After the stromal networks formed through branching and joining with other adjacent cell populations, T-cells were added to the newly formed stromal networks. Here, we demonstrated that T-cells' migration and interaction with the stromal network *in vitro* occurred similar to the T-cell zones of the lymph nodes *in vivo*. By utilizing various mechanical and biological properties of fibrin, collagen, and fibrin–collagen, we have shown that *in vitro* 3D hydrogel-based system can mimic lymphoid stromal networks *in vivo* and can model T-cell interaction in SLOs.

MATERIALS AND METHODS

Cell isolation and culture

Human bone marrow stromal cell line, HS-5 (ATCC CRL-11882), was cultured in DMEM (Dulbecco's modified Eagle's medium) culture medium (ATCC, Manassas, VA) supplemented with 10% heat-inactivated fetal bovine serum (FBS) (Biowest). HS-5 cells, which resemble FRCs in that they are podoplanin-positive and CD31-negative, were cultured in T-75 flasks and split in a 1:5 ratio every 3–4 days. CD4+ T-cells used in this study, P2 cells,[22] were isolated from A3.01 cells (a subclone of the CEM cell line) based on its high propensity to adopt a polarized shape. These T-cells were cultured in RPMI-1640 medium (Gibco, Life Technologies, Grand Island, NY) supplemented with 10% heat-inactivated FBS in T-25 flasks, placed upright, and split in a 1:10 ratio every 3–4 days. All culture media were supplemented with 1% PenStrep (Lonza, Basel, Switzerland) and incubated in 5% CO_2 atmosphere at 37 °C.

Gel preparation and cell encapsulation

Fibrin gel. Dialyzed sterile bovine fibrinogen (Sigma-Aldrich, St. Louis, MO) (12.0 mg/mL), HS-5 cells, and bovine thrombin (Sigma-Aldrich) (50 IU/mL) were mixed and extruded homogeneously using the extruder from the Hemaseel APR Sealer Protein Kit (Haemacure, Sarasota, FL) to obtain a fibrin gel with the final fibrinogen of 6 mg/mL and 220,000 cells/mL gel concentrations. Fibrin gels (each with 200 μL volume) with encapsulated stromal cells were allowed to gel in 48-well plates for 10 min in the incubator (37 °C, 5% CO_2). Fibrin coagulated and formed solid gels after 10 min, and the addition of 200 μL media did not disturb the morphology of the gel. A timeframe of 10 min was selected to maximize the cell viability during the polymerization process. Media was changed every 2 days, and cells were cultured up to 8 days. Each experiment was repeated five times, and the results were reproducible.

Type I collagen gel. Type I Collagen rat tail (Col I) (8.56 mg/mL) (BD Biosciences, San Jose, CA) was mixed with appropriate amounts of 10× PBS, 1*N* NaOH, and dH_2O to make the final concentration of 2 or 4 mg/mL. This was quickly followed by the addition of cells to reach a final concentration of 220,000 cells/mL. Constructs (each with 200 μL volume) were allowed to gel in 48-well plates for 10 min in the incubator (37 °C, 5% CO_2). Collagen coagulated and formed solid gels after 10 min, and the addition of 200 μL media did not disturb the morphology of the gel. Media was changed every 2 days, and cells were cultured up to 8 days. Each experiment was repeated five times, and the results were reproducible.

Fibrin–collagen I gel. To reach a final concentration of 6 mg/mL fibrinogen and 2 or 4 mg/mL type I collagen in a gel, we added the appropriate amounts of Col I (8.56 mg/mL), fibrinogen (12.0 mg/mL), 10× PBS, 1*N* NaOH, dH_2O, and 50 IU/mL bovine thrombin (Sigma-Aldrich). Each concentration of fibrinogen, thrombin, and collagen were selected based on previous *in vitro* 3D cell culture studies,[23–25] which have shown to support cell growth and proliferation. Cells were harvested and resuspended in fibrinogen to reach a final concentration of 220,000 cells/mL. Constructs (each with 200 μL volume) were allowed to gel in 48-well plates for 10 min in the incubator (37 °C, 5% CO_2).

Fibrin–collagen coagulated and formed solid gels after 10 min, and the addition of 200 μL media did not disturb the morphology of the gel. Media was changed every 2 days, and cells were cultured up to 8 days. Each experiment was repeated five times, and the results were reproducible.

Green fluorescent protein transfection

To visualize HS-5 stromal networks up to 8 days in culture and to quantify cell area using fluorescence, HS-5 cells were stably transfected to express green fluorescent protein (GFP). Twenty-four hours prior to transfection, HS-5 cells were seeded in six-well plate to reach 60% confluency on the day of transfection. Plasmid DNA vector (pLenti-III-CMV-GFP-Puro, LV590, Applied Biological Materials, Richmond, BC, Canada) was mixed with Fugene 6 transfection reagent (Promega, Madison, WI) and Opti-MEM (Life Technologies) according to the manufacturer's instructions. DNA/Fugene6/Opti-MEM mixture was added dropwise to the well of the six-well plate containing growth medium. Cells were then incubated at 37 °C for 48 h. The GFP plasmid construct contains a puromycin resistance gene, which allows selecting stably transfected cells by culturing in a medium supplemented with 1 μg/mL puromcyin (Sigma-Aldrich). After 48 h, incubated HS-5 cells were subcultured 1:3 in selection medium. Selection medium was replaced every 3 days for 14 days. Successful selection was confirmed by the observation of 100% distinct colonies of surviving GFP-positive HS-5 cells.

Fluorescent area measurement

A MATLAB code was created using the Image Processing Toolbox to determine the approximate area of GFP-expressing cells. Specifically, the green channel was parsed out from each image before using image segmentation functions to create a gradient picture. Image segmentation relies upon differences in contrast to create a binary mask of the image. Once the binary mask image contained outlines of the cells, the mask was dilated and filled to cover the full area of each cell. Within the binary mask, white spots denoted cells, and cell area was calculated by determining the number of white pixels per image and converting the number to a size in micrometers (Supporting Information Fig. S3). Additionally, the binary mask outline was superimposed onto the original image to ensure that cell area was detected appropriately. All the analyzed images were taken at ×100 magnification by the inverted microscope Leica DMI3000B, and images were screened, selected, and analyzed using a double-blind method ($n = 5$).

Aprotinin test

To slow down fibrinolysis, the culturing media (DMEM with 10% FBS) was supplemented with monomeric serine protease inhibitor, aprotinin (Sigma-Aldrich). Aprotinin was added in the medium to reach and to maintain sufficient concentration levels throughout the 8 days of culture and to be able to easily modify the concentration if necessary. Before addition, 1 TIU/mL aprotinin was diluted with culturing media to the desired aprotinin concentration (0.1 and 0.05 TIU/mL). Aprotinin was added beginning on day 2 and continued until day 8 of culture. At days 4, 6, and 8 of the culture, its effects on HS-5 stromal network formation were examined by measuring the fluorescent cell area as described previously ($n = 5$).

Fibrin degradation assays

To measure the degradation rate of fibrin gels, we mixed unlabeled fibrinogen with AlexaFluor546-labeled fibrinogen (Invitrogen, Carlsbad, CA), resulting in 2% w/w labeling. HS-5 cells were encapsulated in the fluorescently labeled fibrin gels and cultured in DMEM without phenol red and supplemented with 4 m*M* L-Glutamine (ATCC). A plate reader (Fluoroskan Ascent FL, ex. 558/em. 573 nm) was used to measure the levels of soluble degradation products, AlexaFluor conjugate, released from the labeled fibrinogen as a result of the fibrin degradation ($n = 5$). Medium was collected every 2 days for up to 8 days of culture. As a control, we measured the release of the AlexaFluor conjugate to the media from fibrin gels without cells to ensure that the fibrin degradation is driven by the cells. We did not detect a fluorescent signal when fibrin gels were cultured without the cells, and no autofluorescence was detected from the media.

Stromal cell viability

CellTiter-Glo Luminescent Cell Viability Assays (Promega) was used to determine the number of viable cells based on quantification of ATP present, which indicates the presence of metabolically active cells. This procedure was carried out on day 8 for all conditions as described by the manufacturer's protocol. The luminescence values were recorded by using a plate reader (Fluoroskan Ascent FL) after 10 min of incubation at room temperature to stabilize the luminescent signals. Standard curves were generated for each gel condition to identify the linear relationship between the luminescent signal and the number of cells in the hydrogel, ranging from 0 to 2 million cells per gel in the 96-well format ($n = 5$).

T-cell interaction with HS-5 stromal network

Staining T-cells. T-cells were harvested by centrifugation and resuspended in prewarmed CellTracker CMTPX (Invitrogen) at 10 μ*M* working concentration. Cells were then incubated for 30 min under growth conditions. The dye working solution was replaced with fresh media and incubated for another 30 min in 37 °C. Cells were washed with PBS and resuspended with fresh media.

T-cell addition to the hydrogel and microscopy. CellTracker CMTPX-labeled P2 T-cell line (1.1×10^6 cells/mL) was resuspended in DMEM supplemented with 10% FBS and 0.05 TIU/mL aprotinin and added to the HS-5 stromal network in fibrin gel (6 mg/mL) (220,000 cells/mL gel) on day 6 of culture. Twelve hours after CMTPX-labeled P2-T-cells were added in suspension and allowed to sediment, these gels were imaged using Delta Vision-RT Live Cell Imaging System overnight to observe the T-cell migration and

interaction with the stromal network. On day 8, all gels were fixed in 10% formalin (Electron Microscopy Sciences, Hatfield, PA) for 10 min and then carefully washed three times with 1× PBS (Sigma-Aldrich), 50% EtOH, and 70% EtOH, respectively. All images of these fixed gels were taken using confocal microscope Nikon A1 to verify the T-cell interaction with the HS-5 stromal network. Each experiment was performed at least five times, and the result was reproduced.

T-cell viability assay. To assure T-cell viability in HS-5 culturing media (DMEM), T-cells were cultured in both DMEM and RPMI-1640 medium in six-well plates for 2 days. Cells were then stained with LIVE/DEAD Cell Imaging Kit (488/570) (Invitrogen) as described by the manufacturer's protocol. T-cell viability was quantified by dividing the number of dead cells by the total number of cells shown in ×50 images ($n = 2$).

Statistical analysis

All statistical analyses were performed using GraphPad Prism (GraphPad Prism Software, La Jolla, CA). Data are reported as mean ± standard deviation (SD) of measurements, and analyzed with two-way analysis of variance followed by Tukey's post-test. Statistical significance was assumed when $p < 0.05$.

RESULTS

Stromal network formation in fibrin gel

To design a 3D hydrogel system that can support and mimic a lymphoid stromal network, fibrin gel was investigated. The encapsulated HS-5 cells in fibrin gel (6 mg/mL) demonstrated fibroblast-like spindle morphology at day 2, and stromal networks began to form through branching and joining with other adjacent cell populations by day 6 [Fig. 1(A)]. However, because of the rapid fibrinolysis along with cell growth, fibrin degraded completely by day 8, leading to the loss of the structural support and contraction of the stromal network architecture [Fig. 1(A) and Supporting Information Fig. S1]. Inability to maintain the matrix architecture after complete network formation restricted T-cell penetration into the network because of the high density of the cells and the collapse of the fibrin structure.

Optimal aprotinin concentration controls fibrin degradation and cell spreading

We hypothesized that the kinetics of fibrin degradation would affect cell proliferation, migration, and cell-mediated matrix remodeling. We used a monomeric serine protease inhibitor, aprotinin, added to the culturing media to control the fibrin degradation rate and to extend the period when the stromal network architecture is supported. Higher concentration of aprotinin (0.1 TIU/mL) slowed down fibrinolysis significantly [Fig. 1(B,C)], but also restricted cell growth [Fig. 1(A)]. As a result, we concluded that in order for HS-5 cells to proliferate and connect with other surrounding cells, these cells have to be able to migrate and remodel their microenvironment. Reducing the aprotinin concentration to 0.05 TIU/mL resulted in sufficient cell proliferation for network formation, and slow enough fibrin degradation [Fig. 1(A) and Supporting Information Fig. S1].

After identifying the optimal aprotinin concentration that allows both control over fibrinolysis and maintenance of the stromal network, the ability to support cell growth and network formation was assessed quantitatively by measuring the fluorescent area occupied by the cells in the hydrogel [Fig. 1(D)]. Compared with no-aprotinin control condition, fibrin gels supplemented with aprotinin (0.05 TIU/mL) showed slower cell proliferation rate and lower cell area in the beginning stage of culture, which then significantly increased, by day 8 [Fig. 1(D)]. On the other hand, the cell area in fibrin gel without aprotinin slightly decreased at day 8 due to accelerated fibrinolysis and its inability to maintain the architecture lead to the collapse of the stromal network [Fig. 1(D) and Supporting Information Fig. S1]. Only fibrin gel supplemented with aprotinin (0.05 TIU/mL) showed significant increase in normalized fluorescent cell area from day 4 to day 8, proving the importance of a balance between fibrin degradation and cell proliferation in the stromal network formation [Fig. 1(D)]. There was no statistical difference in normalized cell area between fibrin gel supplemented with 0.05 TIU/mL aprotinin and fibrin gel alone throughout any day of the culture; however, the ability to maintain the structural architecture after complete network formation was significantly improved with the addition of 0.05 TIU/mL aprotinin [Fig. 1(A) and Supporting Information Fig. S1].

HS-5 stromal network formation in type I collagen gel

We investigated type I collagen gel as it constitutes bundles along which FRCs form the network in T-cell zones.[1] Based on the results from the aprotinin test with fibrin gels, we hypothesized that compact environments restrict cell growth. Therefore, we investigated high (4 mg/mL) and low (2 mg/mL) collagen concentration to test our hypothesis. In 4 mg/mL collagen gels, HS-5 cells exhibited fibroblast-like spindle morphology at day 4. The growth slowed down by day 8 (Fig. 2, box) in 4 mg/mL collagen gels; however, HS-5 cells showed better growth by day 8 in 2 mg/mL collagen gels than in 4 mg/mL collagen gels (Fig. 2).

HS-5 stromal network formation in fibrin–collagen gel

Based on results from both fibrin and collagen gel, we hypothesized that combining the faster-degrading fibrin and slow-degrading collagen gel would provide optimal degradation rate and structural rigidity to promote cell growth and network formation. Fibrin concentration was kept constant at 6 mg/mL, and only collagen concentration was varied (collagen concentration: 2 mg/mL and 4 mg/mL) to identify the optimal concentration for HS-5 cells. The trend observed in fibrin and collagen gels continued, and HS-5 started to express a fibroblast-like spindle phenotype in both low- and high-collagen fibrin–collagen gels. However, no significant growth or network formation was observed in 4 mg/mL fibrin–collagen gels at day 8 (Fig. 3). Similar to collagen

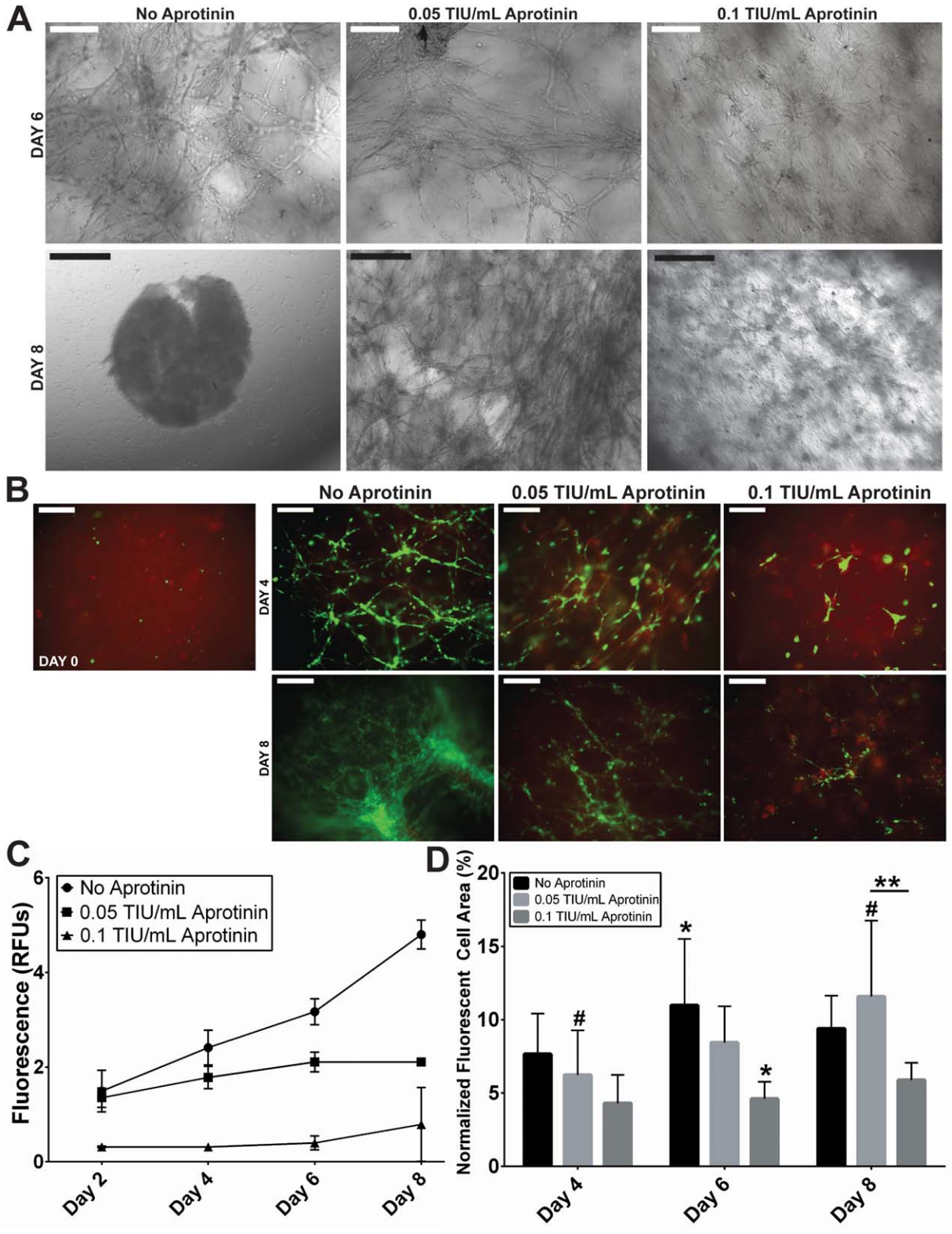

FIGURE 1. Effects of aprotinin on HS-5 stromal network formation and fibrin degradation rate. A: HS-5 cells encapsulated in fibrin (6 mg/mL) gel (220,000 cells/mL gel) and two different concentrations of aprotinin (0.1 and 0.05 TIU/mL) were supplemented with media. Scale bar: white = 200 μm and black = 500 μm. B: GFP-labeled HS-5 were encapsulated in fibrin gels copolymerized with 2% w/w AlexaFluor 546 (558/573 nm) labeled fibrinogen to measure the fibrin degradation during the stromal network formation. Scale bar: 200 μm. C: Fluorescence was measured in the media that was collected every 2 days from fibrin gels labeled with 2% w/w AlexaFluor 546. Stronger fluorescence was detected in media collected from more degraded fibrin gels, verifying the effect of aprotinin concentration on fibrinolysis. Values are reported as mean ± SD ($n = 5$). D: The area occupied by cells was quantified as the area corresponding with GFP fluorescence within ×100 images (Supporting Information Fig. S3). Only fibrin gel supplemented with aprotinin (0.05 TIU/mL) showed significant increase in normalized fluorescent cell area from day 4 to day 8. Values are reported as mean ± SD ($n = 5$). Statistical significance was determined by a two-way analysis of variance followed by Tukey's post-tests (*, **, and # indicate $p < 0.05$). [Color figure can be viewed in the online issue, which is available at wileyonlinelibrary.com.]

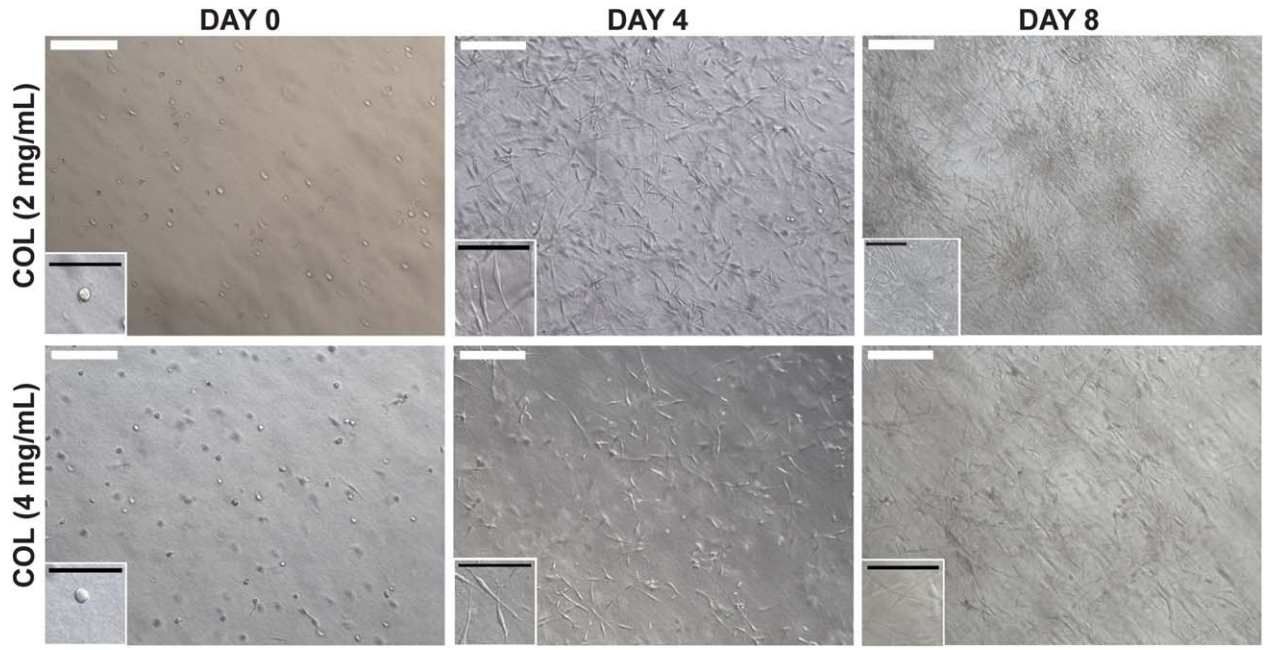

FIGURE 2. Effects of collagen concentration on HS-5 stromal network formation in type I collagen gel. HS-5 cells were encapsulated in type I collagen gel (220,000 cells/mL gel) and 2 mg/mL and 4 mg/mL collagen concentration were compared. The growth slowed down by day 8 in 4 mg/mL collagen gels; however, HS-5 cells showed better growth by day 8 in 2 mg/mL collagen gels than in 4 mg/mL collagen gels. Scale bar: white = 200 μm and black = 100 μm. [Color figure can be viewed in the online issue, which is available at wileyonlinelibrary.com.]

gels, HS-5 cells showed better cell growth in 2 mg/mL fibrin–collagen gels than in 4 mg/mL fibrin–collagen gels (Fig. 3). Fibrin–collagen gels (2 mg/mL) contracted significantly as early as day 2, limiting cell growth and expansion (Supporting Information Fig. S2).

Comparison among three different hydrogel systems: Fibrin, fibrin–collagen, and collagen

After characterizing the degradation rate in the presence of cells in three different hydrogel compositions, we performed a quantitative analysis of the gels' ability to support cell proliferation and

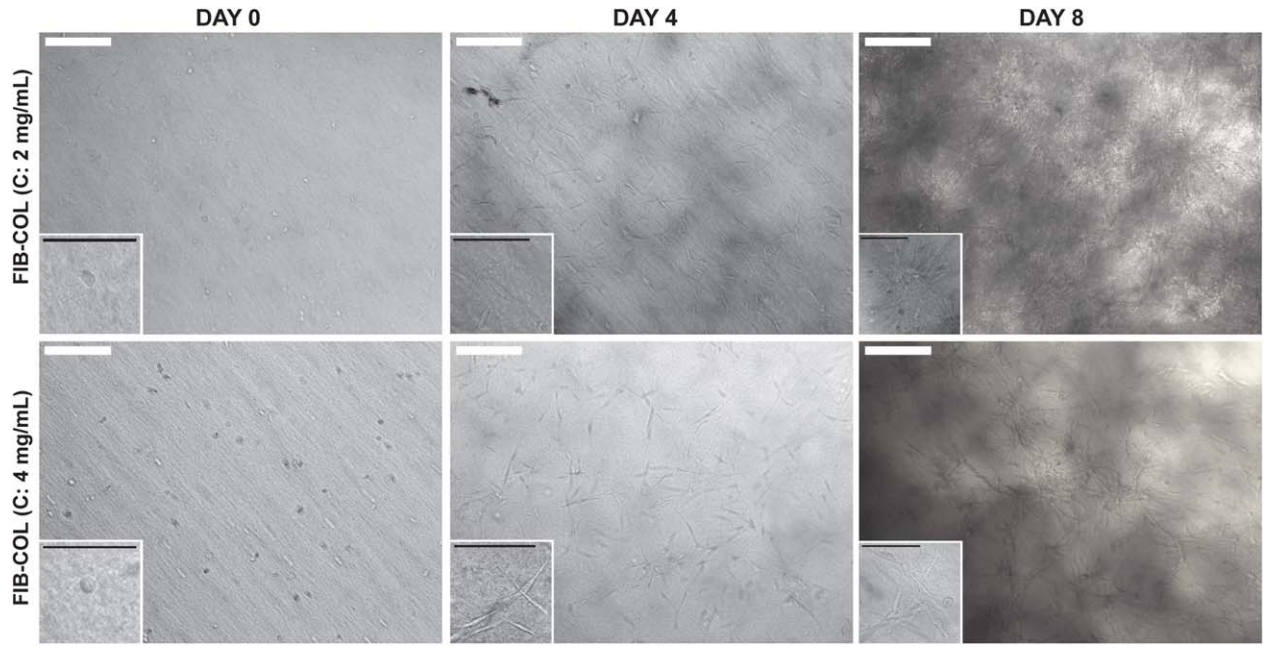

FIGURE 3. Effects of collagen concentration on HS-5 stromal network formation in fibrin–collagen gel. HS-5 cells were encapsulated in fibrin–collagen gel (220,000 cells/mL gel) and 2 mg/mL and 4 mg/mL collagen concentration were compared. As in collagen gels, HS-5 cells showed better cell growth in 2 mg/mL fibrin–collagen gels than in 4 mg/mL fibrin–collagen gels. Scale bar: white = 200 μm and black = 100 μm. [Color figure can be viewed in the online issue, which is available at wileyonlinelibrary.com.]

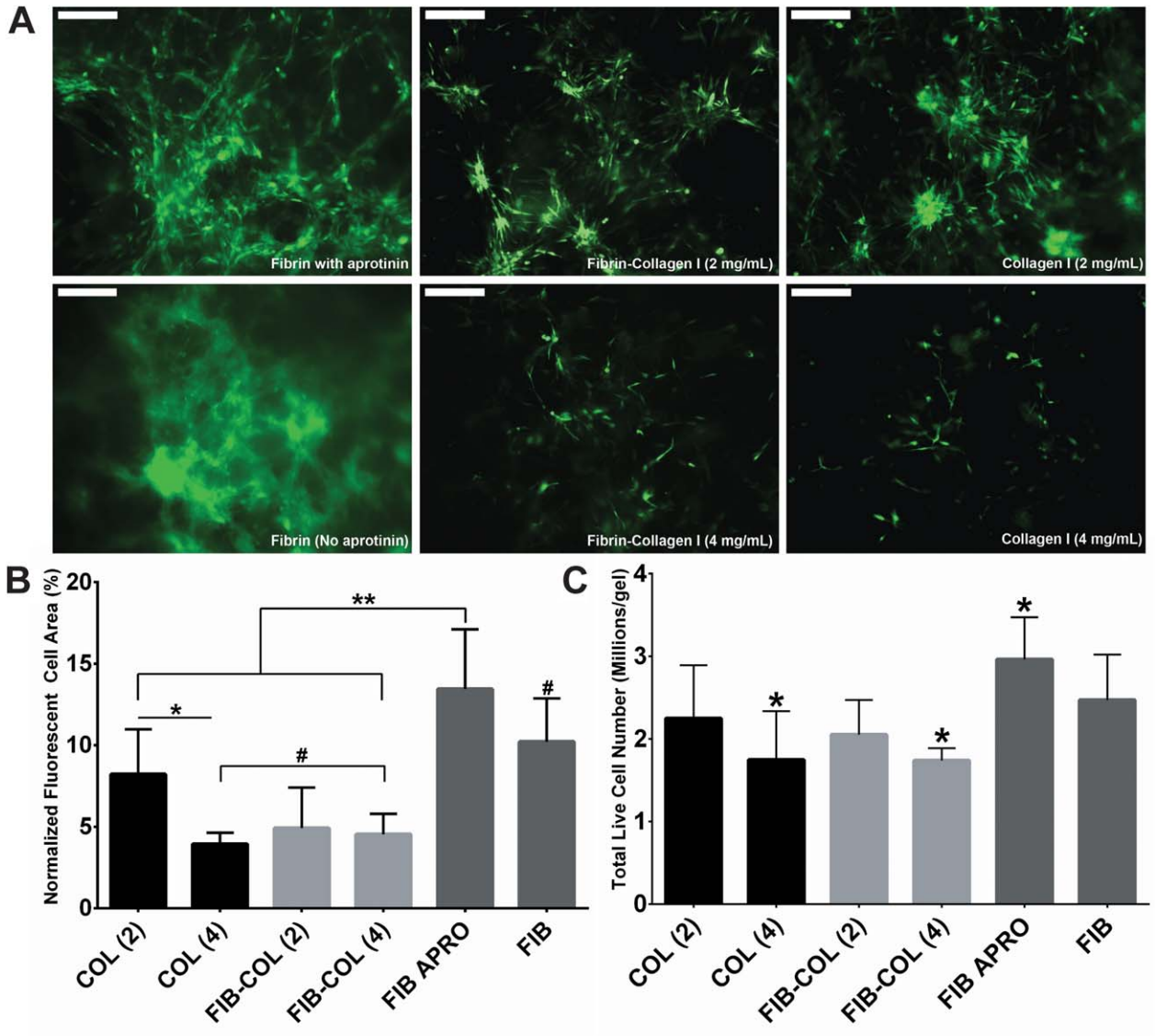

FIGURE 4. Comparison among three different hydrogel systems: fibrin, fibrin–collagen, and collagen. A: GFP-labeled HS-5 cells (220,000 cells/mL gel) encapsulated in six different hydrogel conditions: fibrin with and without aprotinin, fibrin–collagen, and pure collagen at various concentrations. Fibrin concentration was kept at 6 mg/mL for all gels, and only collagen concentration was varied from 2 to 4 mg/mL. HS-5 formed more interconnected and complete network in fibrin gel with aprotinin (0.05 TIU/mL). Scale bar: 200 μm. B: The normalized fluorescent cell area was quantified as the area corresponding with the GFP fluorescence within ×100 images and compared among the different hydrogel systems. Fibrin gel supplemented with aprotinin (0.05 TIU/mL) showed significantly greater values of total cell area at day 8 compared with all compositions of collagen and fibrin–collagen. Values are reported as mean ± SD ($n = 5$). C: CellTiter-Glo luminescent cell viability assay was used to determine the total number of viable cells per gel based on quantification of ATP. Fibrin gel supplemented with aprotinin (0.05 TIU/mL) showed significantly greater values of viable cells at day 8 compared with collagen (4 mg/mL) and fibrin–collagen (4 mg/mL). Values are reported as mean ± SD ($n = 5$). Statistical significance was determined by a two-way analysis of variance followed by Tukey's post-tests (*, **, and # indicate $p < 0.05$). [Color figure can be viewed in the online issue, which is available at wileyonlinelibrary.com.]

network formation. The normalized fluorescent cell areas within images taken at ×100 magnification [Fig. 4(B)] and the overall viable cell number [Fig. 4(C)] at day 8 were assessed for the hydrogels with different collagen concentrations. In general, both the degree of stromal network formation and the number of viable cells clearly increased with decreasing collagen concentration in collagen and fibrin–collagen gels. Fibrin gel supplemented with aprotinin (0.05 TIU/mL) showed significantly higher values of cell area [Fig. 4(B)] as well as viable cell number [Fig. 4(C)] at day 8 compared with all concentrations of collagen and fibrin–collagen, and supported 67-fold increase in the number of viable cells. There was no statistical difference between fibrin gel supplemented with aprotinin and fibrin gel alone in both normalized cell area and viable cell number; however, a dense mass of cells formed in fibrin gel without aprotinin [Fig. 4(A)] because of the collapse of the fibrin structure.

T-cell interaction

Before adding T-cells to the stromal network in fibrin gel, we verified their viability in HS-5 DMEM-based culture

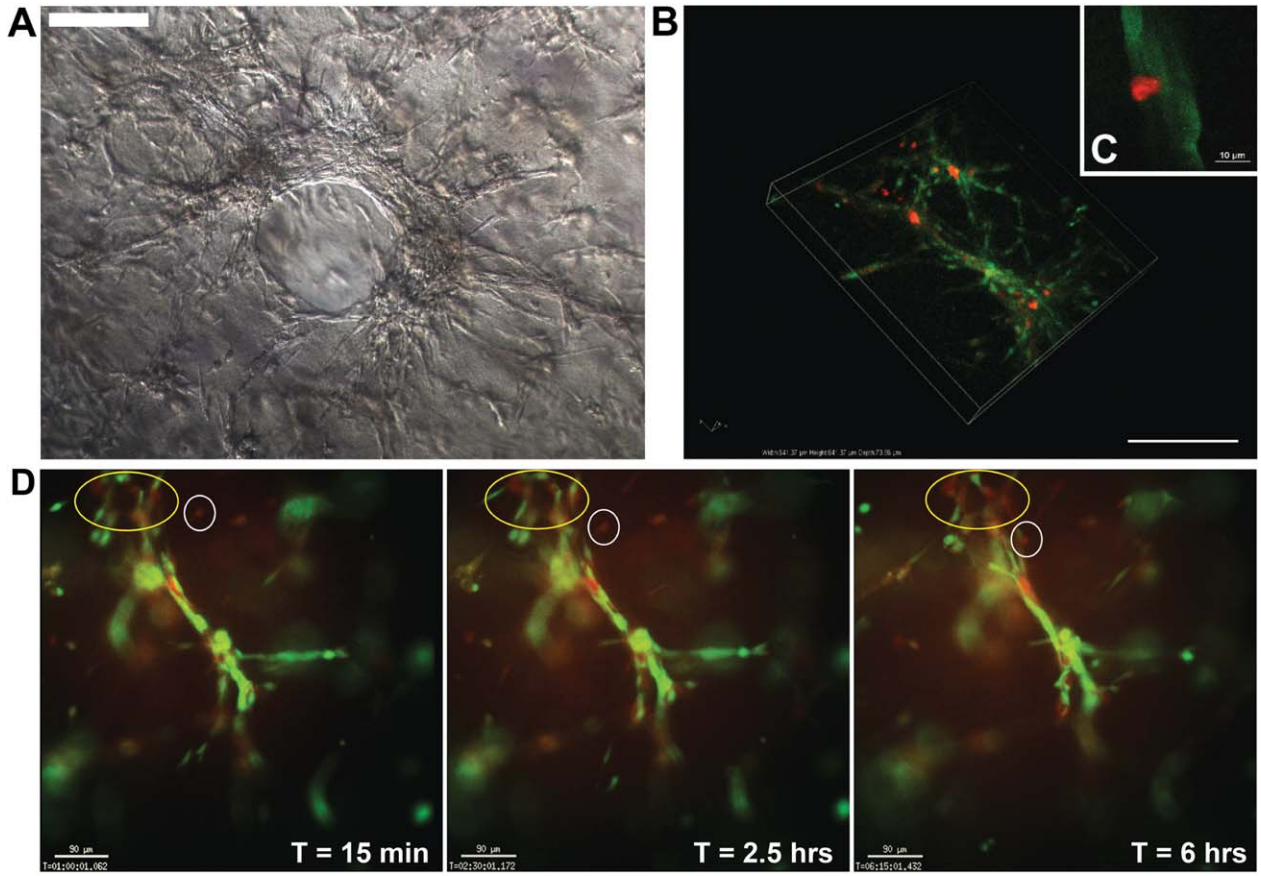

FIGURE 5. T-cell interaction with HS-5 stromal network. A: T-cells (red) were added after complete HS-5 stromal network formation after 6 days of culture. Controlled degradation of fibrin and HS-5 remodeling resulted in the formation of cavities that promoted T-cell infiltration through. Scale bar: 200 μm. B: Two days after addition, T-cell interaction was observed using Nikon A1 confocal microscope. T-cells (red) are visible only along the line of the stromal network (green) confirming T-cell attachment and interaction with the stromal network. Scale bar: 100 μm. C: A single T-cell (red) attachment on the stromal network (green) was confirmed by using Nikon A1 confocal imaging (×900 magnification). Scale bar: 10 μm. D: T-cell migration and interaction with the stromal network were observed using Delta Vision-RT Live Cell Imaging System overnight starting 12 h after T-cells addition (Supporting Information Videos 1 and 2). Twelve hours after T-cell addition, multiple T-cells adhered to stromal networks (yellow circle), and individual T-cell migration toward the stromal cells was still observed (white circle). [Color figure can be viewed in the online issue, which is available at wileyonlinelibrary.com.]

media, because T-cells were cultured in a different culture media than stromal cells (RPMI vs. DMEM) (Supporting Information Fig. S4). T-cells survived and proliferated in DMEM-based media demonstrating that it can support the co-culture of T-cells and HS-5 cells. T-cells labeled with CellTracker CMTPX (1.1×10^6 cells/mL) were added to the stromal network in fibrin gel supplemented with 0.05 TIU/mL aprotinin on day 6 of culture. Stromal cells had remodeled the matrix and degraded the surrounding fibrin gel, creating openings for T-cell migration [Fig. 5(A)]. On the contrary, adding T-cells to the fibrin–collagen and collagen gels did not result in T-cell penetration, and most of the added cells were found on the bottom of the dish. To further verify the T-cell migration and interaction with the stromal network, cells were imaged using confocal microscopy at day 8 [Fig. 5(B,C)] and observed using Delta Vision-RT Live Cell Imaging System overnight starting 12 h after T-cells addition [Fig. 5(D) and Supporting Information Videos 1 and 2]. Twelve hours after T-cell addition, multiple T-cells adhered to stromal networks [Fig. 5(D), yellow circle] and individual T-cell migration toward the stromal cells was observed [Fig. 5(D), white circle]. Two days after T-cell addition, T-cells were visible only along the line of the stromal network, confirming T-cell attachment and interaction with the stromal network [Fig. 5(B,C)], similar to the T-cell zones in the lymph nodes *in vivo*.[6]

DISCUSSION

The goal of this study was to create a 3D hydrogel system that can support lymphoid stromal network formation similar to *in vivo* to study T-cell interaction in SLOs. Natural hydrogels provide a 3D mechanical and biochemical environment and allow interaction among embedded cells due to their endogenous biological activity. Fibrin and collagen gels undergo cell-mediated degradation through cell-secreted enzymes, such as plasmin and matrix metalloproteinase, allowing cell migration, proliferation and remodeling of the encapsulating matrix.[10] We have characterized each hydrogel system and its ability to support the 3D

stromal network formation. Among the different gel systems, more cell growth and more interconnected stromal network formation were observed when cells were in less rigid and more degradable environments, allowing branching and cell remodeling. The fast degradation rate of fibrin can be controlled with aprotinin, making it a potential material for *in vitro* 3D hydrogel system. High concentration of aprotinin slowed down fibrinolysis significantly; however, it slowed down cell growth as well. In order for cells to proliferate and connect with other surrounding cells, these cells have to be in a microenvironment where they can migrate and remodel. After reducing the aprotinin concentration to 0.05 TIU/mL, the level of proliferation and network formation were recovered while slowing down the fibrin degradation.

To better mimic the *in vivo* microenvironment, we further investigated fibrin–collagen by incorporating naturally degradable fibrin into collagen gel to allow more cell growth and better stromal network support. Surprisingly, fibrin–collagen showed lower values of normalized fluorescent cell area and viable cell number compared with both pure fibrin and collagen. This could be due to the overall mechanics of fibrin–collagen and collagen gels being influenced by changes in the network architecture. Multiple studies have shown the trend of increase in the stiffness of fibrin–collagen compared with that of pure fibrin or collagen gel.[23–25] Depending on protein concentrations, the storage modulus of the gel varied; however, the trend of fibrin–collagen having a greater modulus compared with pure fibrin or collagen was consistent throughout these studies. The increase in the microstructure stiffness is likely due to the greater amount of protein in fibrin–collagen gels and the combinatory effect of highly connected bundles of collagen and interfibrillar bonding of fibrin.[24,26] Also, it has been shown that the permeability correlates with the overall collagen content and decreased collagen concentration resulted in an increase in overall permeability,[27] which allowed better T-cell infiltration.

Gel contraction of both collagen and fibrin–collagen gels over time also could have restricted stromal cell growth and network formation. Collagen-containing gels are known to contract over time due to cells attaching and pulling on fibers as well as the force generated from cell-to-cell contact.[11,28] Fibrin–collagen underwent more significant contraction compared with pure collagen gels as fibrin degraded away. Fibrin gel also contracted, but the addition of optimal aprotonin concentration resulted in balanced matrix degradation and cell proliferation. The controlled cell-mediated degradation in this specific combination created openings that allowed T-cells to penetrate through, which makes it more suitable for T-cell migration and interaction studies.

We have verified T-cell migration and interaction with the stromal network using confocal microscopy and live cell imaging; however, further studies will be necessary to identify whether T-cell migration and trafficking depend on stromal cell expression of CCL19,[2] CCR 21,[29] or adhesion ligands like ICAM-1,[30] which is what occurs in T-cell zones. *In vivo*, the majority of T-cells enters and migrates through and exits the SLOs continuously to seek infected cells in the organism,[2] which is not accurately represented in our system. However, considering that T-cell recruitment and migration *in vivo* is a complicated process, we believe that our 3D system can function as a useful tool to identify factors involved in T-cell–T-cell and T-cell–stromal-cell interactions in SLOs. One possible application of these 3D hydrogel systems would be to model cell–cell interactions in SLOs and study the role of these interactions in cell-to-cell HIV transmission *in vivo*.

CONCLUSION

In summary, by utilizing and characterizing natural hydrogels like fibrin, fibrin–collagen, and collagen, we developed 3D hydrogel systems *in vitro* that can mimic lymphoid stromal networks as assembled *in vivo* and eventually allow us to model T-cell interaction in SLOs. Throughout the different gel systems, more cell growth and more interconnected stromal network formation were observed when cells were in less rigid and more degradable environments, which allowed branching and cell remodeling. Unlike slow degrading collagen-containing gel systems, fibrin degradation rate can be controlled with aprotinin, making this the ideal hydrogel system. We have verified T-cell interaction with the stromal network constructed within fibrin gels supplemented with aprotinin using confocal imaging and live cell imaging; however, further studies would be necessary to identify whether T-cell migration and trafficking depend on stromal cell expression of CCL19 or CCL21 as observed in T-cell zones of SLOs. We believe that the described 3D hydrogel system can help identify cellular factors modulating T-cell behavior in SLOs as well as the cell-to-cell HIV transmission mechanism in lymphoid organs and serve as a complementary approach to the *in vivo* multiphoton imaging.

ACKNOWLEDGMENTS

No benefit of any kind was received either directly or indirectly by the author(s).

REFERENCES

1. Junt T, Scandella E, Ludewig B. Form follows function: Lymphoid tissue microarchitecture in antimicrobial immune defence. Nat Rev Immunol 2008;8:764–775.
2. Masopust D, Schenkel JM. The integration of T cell migration, differentiation and function. Nat Rev Immunol 2013;13:309–320.
3. Roozendaal R, Mebius RE. Stromal cell-immune cell interactions. Annu Rev Immunol 2011;29:23–43.
4. Randall TD. Stromal cells put the brakes on T-cell responses. Immunol Cell Biol 2012;90:469–470.
5. Gretz JE, Anderson AO, Shaw S. Cords, channels, corridors and conduits: Critical architectural elements facilitating cell interactions in the lymph node cortex. Immunol Rev 1997;156:11–24.
6. Bajenoff M, Egen JG, Koo LY, Laugier JP, Brau F, Glaichenhaus N, Germain RN. Stromal cell networks regulate lymphocyte entry, migration, and territoriality in lymph nodes. Immunity 2006;25:989–1001.
7. Yamada Y, Kleinman HK. Functional domains of cell adhesion molecules. Curr Opin Cell Biol 1992;4:819–823.

8. Kaibara M, Fukada E. Effect of temperature on dynamic viscoelasticity during the clotting reaction of fibrin. Biochim Biophys Acta 1977;499:352–361.
9. Blomback B, Carlsson K, Fatah K, Hessel B, Procyk R. Fibrin in human plasma: Gel architectures governed by rate and nature of fibrinogen activation. Thromb Res 1994;75:521–538.
10. Mosesson MW. Fibrinogen and fibrin structure and functions. J Thromb Haemost 2005;3:1894–1904.
11. McGuigan AP, Bruzewicz DA, Glavan A, Butte MJ, Whitesides GM. Cell encapsulation in sub-mm sized gel modules using replica molding. PLoS One 2008;3:e2258.
12. Lee CH, Singla A, Lee Y. Biomedical applications of collagen. Int J Pharm 2001;221:1–22.
13. Hesse E, Hefferan TE, Tarara JE, Haasper C, Meller R, Krettek C, Lu L, Yaszemski MJ. Collagen type I hydrogel allows migration, proliferation, and osteogenic differentiation of rat bone marrow stromal cells. J Biomed Mater Res A 2010;94:442–449.
14. Naito H, Yoshimura M, Mizuno T, Takasawa S, Tojo T, Taniguchi S. The advantages of three-dimensional culture in a collagen hydrogel for stem cell differentiation. J Biomed Mater Res A 2013;101:2838–2845.
15. Sigal A, Kim JT, Balazs AB, Dekel E, Mayo A, Milo R, Baltimore D. Cell-to-cell spread of HIV permits ongoing replication despite antiretroviral therapy. Nature 2011;477:95–98.
16. Hubner W, McNerney GP, Chen P, Dale BM, Gordon RE, Chuang FY, Li XD, Asmuth DM, Huser T, Chen BK. Quantitative 3D video microscopy of HIV transfer across T cell virological synapses. Science 2009;323:1743–1747.
17. Baker BM, Chen CS. Deconstructing the third dimension: How 3D culture microenvironments alter cellular cues. J Cell Sci 2012;125: 3015–3024.
18. Schmalstieg FC, Rudloff HE, Hillman GR, Anderson DC. Two-dimensional and three-dimensional movement of human polymorphonuclear leukocytes: Two fundamentally different mechanisms of locomotion [corrected]. J Leukoc Biol 1986;40:677–691.
19. Murooka TT, Deruaz M, Marangoni F, Vrbanac VD, Seung E, von Andrian UH, Tager AM, Luster AD, Mempel TR. HIV-infected T cells are migratory vehicles for viral dissemination. Nature 2012; 490:283–287.
20. Crisa L, Cirulli V, Ellisman MH, Ishii JK, Elices MJ, Salomon DR. Cell adhesion and migration are regulated at distinct stages of thymic T cell development: The roles of fibronectin, VLA4, and VLA5. J Exp Med 1996;184:215–228.
21. Schor SL, Allen TD, Winn B. Lymphocyte migration into three-dimensional collagen matrices: A quantitative study. J Cell Biol 1983;96:1089–1096.
22. Llewellyn GN, Hogue IB, Grover JR, Ono A. Nucleocapsid promotes localization of HIV-1 gag to uropods that participate in virological synapses between T cells. PLoS Pathog 2010;6:e1001167.
23. Rao RR, Peterson AW, Ceccarelli J, Putnam AJ, Stegemann JP. Matrix composition regulates three-dimensional network formation by endothelial cells and mesenchymal stem cells in collagen/fibrin materials. Angiogenesis 2012;15:253–264.
24. Rowe SL, Stegemann JP. Interpenetrating collagen-fibrin composite matrices with varying protein contents and ratios. Biomacromolecules 2006;7:2942–2948.
25. Lai VK, Lake SP, Frey CR, Tranquillo RT, Barocas VH. Mechanical behavior of collagen-fibrin co-gels reflects transition from series to parallel interactions with increasing collagen content. J Biomech Eng 2012;134:011004.
26. Lewis JL, Johnson SL, Oegema TR Jr. Interfibrillar collagen bonding exists in matrix produced by chondrocytes in culture: Evidence by electron microscopy. Tissue Eng 2002;8:989–995. Dec;
27. Helm CL, Zisch A, Swartz MA. Engineered blood and lymphatic capillaries in 3-D VEGF-fibrin-collagen matrices with interstitial flow. Biotechnol Bioeng 2007;96:167–176.
28. Roy P, Petroll WM, Chuong CJ, Cavanagh HD, Jester JV. Effect of cell migration on the maintenance of tension on a collagen matrix. Ann Biomed Eng 1999; 27:721–730.
29. Haessler U, Pisano M, Wu M, Swartz MA. Dendritic cell chemotaxis in 3D under defined chemokine gradients reveals differential response to ligands CCL21 and CCL19. Proc Natl Acad Sci U S A 2011;108:5614–5619.
30. Schumann K, Lammermann T, Bruckner M, Legler DF, Polleux J, Spatz JP, Schuler G, Forster R, Lutz MB, Sorokin L, Sixt M. Immobilized chemokine fields and soluble chemokine gradients cooperatively shape migration patterns of dendritic cells. Immunity 2010;32:703–713.